ACS APPLIED MATERIALS & INTERFACES

Research Article

www.acsami.org

Cross-Linked Polyelectrolyte Multilayers for Marine Antifouling Applications

Xiaoying Zhu,[†] Dominik Jańczewski,*[,†] Serina Siew Chen Lee,[‡] Serena Lay-Ming Teo,[‡] and G. Julius Vancso*[,§,∥]

[†]Institute of Materials Research and Engineering, A*STAR (Agency for Science, Technology and Research), 3 Research Link, Singapore 117602

[‡]Tropical Marine Science Institute, National University of Singapore, 18 Kent Ridge Road, Singapore 119227

[§]Institute of Chemical and Engineering Sciences, A*STAR, 1, Pesek Road, Jurong Island, Singapore 627833

[∥]MESA+ Institute for Nanotechnology, Materials Science and Technology of Polymers, University of Twente, P.O. Box 217, 7500 AE Enschede, the Netherlands

Supporting Information

ABSTRACT: A polyionic multilayer film was fabricated by layer-by-layer (LbL) sequential deposition followed by cross-linking under mild conditions on a substrate surface to inhibit marine fouling. A novel polyanion, featuring methyl ester groups for an easy cross-linking was used as a generic solution for stabilization of LbL films in a harsh environment. Covalent cross-linking was confirmed by FTIR and XPS spectroscopy. AFM was used to observe film morphology and its variation because of cross-linking, as well as to measure the thickness of the LbL films. Cross-linking improved the stability of the LbL film when it was immersed in artificial seawater, natural seawater, and in a polar organic solvent (DMSO). No changes in the thickness and topography of the film were observed in these media. The LbL films prevented settlement of *Amphibalanus amphitrite* barnacle cyprids and reduced adhesion of the benthic diatom *Amphora coffeaeformis*. Assay results indicated that the cross-linking process did not weaken the antifouling effect of LbL films. The high stability and low degree of fouling make these coatings potentially promising candidates in marine applications.

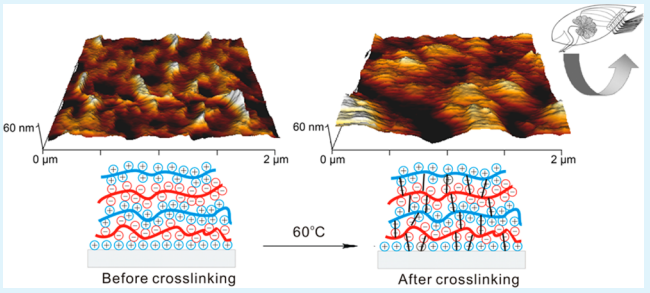

KEYWORDS: *marine fouling, polyelectrolyte, layer by layer assembly, covalent cross-linking*

1. INTRODUCTION

When submerged in seawater, artificial and natural surfaces tend to accumulate undesirable biological growth in a process referred to as biofouling.[1,2] The first stage of fouling involves rapid accumulation of proteins, followed by deposition of microorganisms, such as bacteria, diatoms, spores of micro-algae. It is usually assumed that larger macrofouling organisms settle on these biofilms in the final stage of the process.[3] Marine biofouling incurs substantial costs to maritime industry. For instance, the overall economic impact of hull fouling on a midsized naval surface ship has been estimated to be on the order of $56 M per year.[4] It is also a major problem for harbor installations, oil rigs, underwater sensors, pipelines, and other artificial structures. For example, the accuracy and reliability of underwater sensors may be seriously hampered as a result of biofouling over the surfaces, which transmit signals. Biofouling can block valves, orifices, and other constricted places, when it occurs in pipes and conduits used to conduct seawater in ships, as well as pipes in industrial installations onshore.[5]

In the past, marine fouling was prevented mainly by using coatings loaded with slowly released biocides. As a result of environmental concerns related to the widespread use of tributyl tin (TBT), a common biocide used in many paints, the International Maritime Organization (IMO) banned the use of organotins in marine coatings since January 2003.[6] In addition, legislative controls in many countries, such as the EU Biocide Products Directive, have resulted in restrictions in the use of leachable biocides on marine coatings. This has generated the current wave of interest in research to provide alternative environmental friendly preventive approaches.

Marine biofouling is highly affected by substrate surface properties,[7,8] such as topography (or morphology),[9,10] roughness,[11] surface free energy,[12,13] and surface charge.[5] Electrostatic attraction plays an important role in the initiation of marine fouling, since most of the foulants that can attach to the substrate surface are charged particles, such as bacteria and proteins.[3,14] As a result, various approaches have been attempted to modify the charge of the substrate surfaces to prevent the initial attachment of foulants. One of the most studied approaches is by using zwitterionic polymers, which are

Received: January 22, 2013
Accepted: June 19, 2013
Published: June 19, 2013

   dx.doi.org/10.1021/am4015549 | ACS Appl. Mater. Interfaces 2013, 5, 5961−5968

highly hydrated structures but possess a zero net charge. There are various examples of this approach, used for marine antifouling[13] and protein adhesion prevention.[15,16]

Similar to zwitterionic polymer surfaces, the alternating deposition of oppositely charged polyelectrolytes known as electrostatic layer-by-layer (LbL) technique, also results in formation of a highly hydrated film of self-compensated polyelectrolytes with no counterions within its structure.[17,18] The LbL assembly is a convenient, cheap, and fast method to prepare polymeric films, which can be carried out by alternating dipping the substrates in oppositely charged polyelectrolyte solutions or by spraying these solutions onto the surface.[19] The method has been used to prepare materials for various applications.[20−22] In addition, it has been proved to be particularly useful when enhanced control over the film thickness is desired.

Thin polymer films obtained by the LbL technique have been used to prevent protein adsorption and bacteria fouling. Polyelectrolyte multilayers assembled with poly(allylamine hydrochloride) (PAH) and poly(sodium 4-styrene sulfonate) (PSS) exhibited antimicrobial property without the addition of specific biocides.[23] Zwitterionic sulfobetaine methacrylate was copolymerized with acrylic acid and LbL deposited with polyethylenimine (PEI) onto polymeric substrates to resist platelet adhesion.[15,24] LbL films formed by alternate deposition of a block copolymer comprising PSS and highly hydrophilic poly(poly(ethylene glycol) methyl ether acrylate) (PSS-b-PEG) and PAH exhibited low protein and cell binding characteristics.[25]

Research using LbL assembled thin films for marine antifouling applications is however in its infancy. Covalent LbL surfaces prepared by PEG-modified and "click" amendable polymers have been demonstrated to have antifouling properties against algae and barnacles.[26] Covalent LbL approach requires specialized, sophisticated macromolecules, and may not result in films with net zero charge. Electrostatic LbL multilayers consisting of oppositely charged poly(acrylic acid) and PEI after modification with PEG and tridecafluoroctyltriethoxysilane have been used to reduce the attachment of spores of green alga Ulva.[27] Antifouling in this case was related to the rough film morphology achieved in the deposition process, rather than related to the molecular characteristics of the LbL film itself. Liu at al. used electrostatically assembled LbL films to produce antifouling coatings, however LbL multilayers served only as a scaffold for the deposition of a superhydrophobic top layer, and to support antibacterial nanoparticles in a rather complex system.[28]

As seawater is a highly corrosive environment, attaining stability of the deposited LbL films is a key factor to achieve long-term performance. Covalent cross-linking is the most widely used method to improve the stability of the deposited polyelectrolyte films. For example, PSS/PAH microcapsules were chemically cross-linked with glutaraldehyde.[29] High-energy electromagnetic waves, such as UV radiation have also been used to cross-link poly(acrylic acid-*graft*-azidoaniline) with PEI.[15] In addition, poly(acrylic acid) and PEI LbL films were cross-linked at high temperature (160 °C) and in high vacuum (4×10^{-2} mbar) to form stabilizing amide bonds.[27]

In a present study, a novel polyanion (**P1**) was proposed, which can be easily cross-linked with amines under mild conditions to form a stable covalent bond without the use of any other chemical agent and without high energy radiation. Polyelectrolyte multilayers were fabricated on silicon wafers via LbL assembly to deposit these polyions at substrate surfaces. The cross-linking reaction was verified with FTIR and XPS spectroscopy. The morphology and thickness of the deposited multilayers were observed with AFM. The antifouling performance of the polyelectrolyte multilayers was evaluated in laboratory tests against two common marine fouling organisms including benthic diatoms (*Amphora coffeaeformis*) and barnacle cyprids (*Amphibalanus amphitrite*). These organisms have been previously used in lab assays to evaluate the antifouling properties of various materials.[5,27,30−34]

2. EXPERIMENTAL SECTION

2.1. Materials and Instruments. Poly(isobutylene-*alt*-maleic anhydride) (PIAMA, M_w = 60 000 D), polyethylenimine (PEI, M_w = 25 000 D, branched), 3-aminopropyltrimethoxysilane, 4-(dimethylamino)pyridine (DMAP), and sodium hydroxide were provided by Sigma Aldrich. Solvents including *N*,*N*-dimethylformamide (DMF), dimethylsulfoxide (DMSO), toluene, methanol, and ethanol were purchased from Tedia. Dialysis membrane tubing (MWCO = 12 000−14 000) was received from Fisher Scientific. Silicon wafers were obtained from Latech Scientific Supply Pte. Ltd. Ultrapure water produced by a Millipore Milli-Q integral water purification system was used to prepare aqueous solutions. A triple P plasma processor (Duratek, Taiwan) was used to clean the silicon wafers. NMR (Bruker, 400 MHz), FTIR (Perkin-Elmer), and XPS (VG ESCALAB 250i-XL spectrometer) were used to characterize polymer samples and LbL films. Dynamic light scattering (DLS, Brookhaven Instruments Corp, U.S.A.) was used to measure the size distribution of polymer aggregates.

2.2. Synthesis of the Polyanions (P1 and P2). *Polymer P1.* One gram of PIAMA (IR spectra 1858 and 1777 cm^{-1}) and DMAP (0.026 g) as the catalyst were dissolved in 10 mL of DMF with 500 rpm magnetic stirring at 65 °C. Subsequently, the polymer was completely dissolved and methanol (50 μL) was added to the solution to start the reaction. After 5 h, the polymer solution was slowly poured into 100 mL of NaOH aqueous solution (10 g/L) with 500 rpm magnetic stirring at room temperature. When the solution became clear, it was transferred into the dialysis membrane tubing (1 m) and dialyzed against ultrapure water for 3 days whereby water was changed in every 12 h. The purified aqueous polymer solution was then concentrated by rotary evaporator and finally freeze-dried to get the solid polyanion **P1** (1.11 g, yield 79.3%). NMR calculated Mn: 84 kDa. ^{1}H NMR integrated for a single repeating unit: (D_2O) δ_H: 1.07 (6 H, m), 1.59 (0.48 H, bs), 2.00 (0.94 H, bs), 2.47 (0.70 H, bs), 2.74 (0.79 H, bs), 3.67 (0.25 H, s). IR: 1788, 1731, 1580, 1471, 1396 cm^{-1}.

Polymer P2. PIAMA (1 g) was dissolved in 100 mL of NaOH aqueous solution (10 g/L) with 500 rpm magnetic stirring at room temperature. The polymer was purified the same way as polymer **P1** resulting in a white solid product **P2** (1.16 g, yield 82.4%). NMR calculated Mn: 84.2 kDa. ^{1}H NMR integrated for a single repeating unit: (D_2O) δ_H 1.05 (6 H, m), 1.56 (0.96 H, m), 1.95 (0.94 H, s), 2.38 (0.97 H, m), 2.72 (0.98 H, m). IR: 1582, 1470, 1371 cm^{-1}.

2.3. Assembly and Characterization of the LbL Multilayers. Silicon wafers were cut into 2 cm × 2 cm pieces using a DISCO dicing machine (DAD 321). After ultrasonic cleaning with water and ethanol for 10 min, the pieces were dried over a nitrogen gas stream and treated by oxygen plasma (200 W) for 2 min. The treated silicon wafers were immersed into the 3-aminopropyltrimethoxysilane toluene solution (10 mM) for 5 h to impart positively charged amino groups on the substrate surface.

The pretreated silicon wafers with positive charges were immersed into the aqueous polyanion solution (1 mg/mL) for 10 min, followed by rinsing with ultrapure water for 2 min. Subsequently, they were immersed into PEI aqueous solution (1 mg/mL) for 10 min, followed by another 2 min ultrapure water rinse. The cycle was repeated until the desired bilayer number was reached. For film stability measurements and antifouling performance tests, 6-bilayer structures were employed. The silicon wafers with the deposited LbL films were dried

by nitrogen stream and subsequently under vacuum at room temperature for 5 h. The cross-linking process was conducted by heating the silicon wafers with the dried LbL films to 60 °C for 5 h under vacuum. The deposited LbL films were analyzed by FTIR and X-ray photoelectron spectroscopy (XPS) before and after cross-linking. The FTIR measurements were taken using a Perkin-Elmer FTIR spectroscopy with an attenuated total reflection component using a ZeSe crystal. The XPS spectra of the deposited LbL films were obtained with a VG ESCALAB 250i-XL spectrometer using an Al Kα X-ray source (1486.6 eV photons). XPS data processing, including peak assignment and peak fitting (fitting algorithm Simplex), was done using the software package Thermo Avantage, version 4.12 (Thermo Fisher Scientific). Surface morphology and thickness of the deposited LbL films were measured by a Bruker's Dimension Icon atomic force microscope (AFM) system in the tapping mode. AFM images were taken on dried films with an area of 2 μm × 2 μm for morphology observations and roughness measurements. The film thickness was measured by scratching the multilayer assembly with a fresh razor blade to expose the bare substrate (silicon) and then scanning it with an area of 10 μm × 10 μm to reveal a clear step at the scratch.[35] The height difference between the thin film surface and the bare substrate was considered as the thickness of the thin film, as shown in Table S1 in the Supporting Information. Five sections crossing of a single scratch were used to measure the height differences. The calculated mean value of the height differences was used as the film thickness. AFM raw data was processed by software NanoScope Analysis, Bruker.

Stability of the deposited LbL films, before and after cross-linking, was evaluated in seawater and in a polar organic solvent. The silicon wafers with six bilayers were immersed in artificial seawater prepared with sea salt (40 g/L, Sigma), in natural tropical seawater by immersing coupons in the sea off the West Coast of Singapore, and DMSO for up to 7 days. For the field immersion test, the coupons were secured to frames, and suspended at a depth of 0.5 m.

Samples were removed and rinsed with ultrapure water following 1, 3, 5, and 7 day immersions. After drying under vacuum at room temperature for 5 h, the thickness of the film on the silicon wafer was measured following the method described above. The morphologies of the LbL films were also directly observed when immersed in artificial seawater (ASW) solution using a liquid AFM cell (JPK, NanoWizard 3 NanoOptics).

2.4. *Amphora* Adhesion Assay. *Amphora* species are the most commonly encountered raphid diatoms found in biofilms on submerged surfaces and as such is often used in antifouling tests.[36] *Amphora coffeaeformis* (UTEX reference number B2080) was maintained in F/2 medium[37] in tissue culture flasks at 24 °C under a 12 h light: 12 h dark regime for at least a week prior to use. The algae were gently removed from culture flasks with cell scrapper and clumps were broken up by continuous pipetting and filtering through a 35 μm nitex mesh. The cell count was determined with a hemocytometer and a suspension containing 10 000 cells per mL was made up in 3% salinity, 0.22 μm filtered seawater (FSW). Silicon wafer controls, silicon wafers with LbL films, with and without cross-links were placed randomly in each well, in 6-well Nunc multiwell culture plates, with 8 replicates for each treatment. To each well, 5 mL of algal cell suspension was added. The experiment was allowed to incubate for 24 h in a 12 h light: 12 h dark cycle at 24 °C. At the end of the incubation period, all slides were gently dipped in a beaker of 3% salinity, 0.22 μm FSW to rinse off any unattached cells. This rinse step was repeated three times. Slides were then allowed to air-dry. The slides were examined under an epi-fluorescence microscope. Ten random fields of view were scored at 20× magnifications (0.916 mm^2 per field of view) for each slide.

2.5. Barnacle Settlement Assay. *Amphibalanus amphitrite* barnacle larvae were spawned from adults collected from the Kranji mangrove, Singapore. The nauplius larvae were fed with an algal mixture 1:1 v/v of *Tetraselmis suecica* (CSIRO Strain number CS-187) and *Chaetoceros muelleri* (CSIRO Strain number CS-176) at a density of ~5 × 10^5/mL, and reared at 27 °C in 2.7% salinity, 0.2 μm filtered seawater. Nauplii metamorphosed into cyprids in 5 days and cyprids were aged for minimum of 2 days at 4–6 °C prior to use in settlement assays.[38] As a result of the inherent hydrophilicity of the cleaned silicon wafer, it was difficult to apply the sessile droplet assay for cyprid settlement, as has been reported by Petrone et al..[39] To evaluate the antibarnacle settlement properties of the untreated and LbL filmed silicon wafers, an experiment was set up wherein 4 day old cyprids were contained in a 50 μm Nitex mesh shaped to form a well aproximately 16 cm in diameter with maximum depth of 5 cm, and enclosing a volume of approximately 1 L of seawater (2.7%, 0.22 μm filtered). Maréchal and Hellio had demonstrated that *Semibalanus balanoides* cyprids would not settle on 150 μm nitex mesh.[39] In our study, we observed that cyprids of *A. amphitrite* did not settle on 50 μm nitex mesh. A total of 3000 cyprids were added into the enclosed net to give a concentration of approximately 3 cyprids per mL. Untreated and LbL polyion film covered silicon wafers (8 pieces each) were suspended in this cyprid culture and incubated in the dark at 27 °C for 24 h. A small pinhole was provided at one edge of each wafer and the wafers were hung vertically, suspended with a nylon thread, arranged in a random block design. After 24 h, the coupons were removed. The silicon wafers were photographed and the number of attached and settled cyprids on each piece of silicon wafers was counted.

3. RESULTS AND DISCUSSION

3.1. Characterization of the Polyanions. To achieve improved stability of electrostatic LbL assemblies in a corrosive marine environment, a cross-linkable polyelectrolyte was investigated. The novel polyanion was synthesized through partial alcoholysis of a polyanhydride (PIAMA), (Scheme 1).

Scheme 1. Synthesis of Polymers P1 and P2[a]

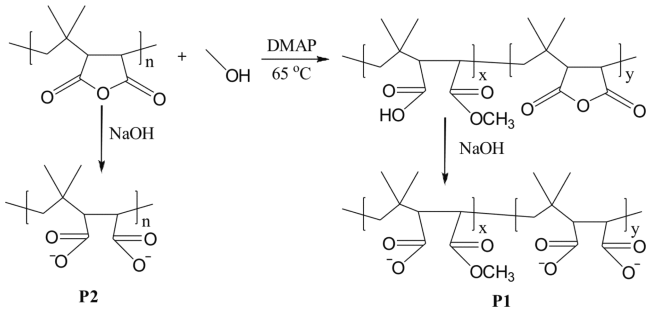

[a] n = 390 (based on the supplier specification), x = 30, y = 360, calculated from NMR.

PIAMA is a suitable commercial precursor and can be easily functionalized with any nucleophilic agents, to produce a wide variety of functional anionic macromolecules.[40] Upon introduction of methyl esters, the rest of the anhydride groups were hydrolyzed by NaOH as shown in Scheme 1. In this way polymer **P1** with methyl ester groups, intended for cross-linking, and carboxylic groups for providing anionic character and water solubility was synthesized. Parallel PIAMA was directly hydrolyzed by NaOH to produce polyanion **P2**, used as a reference.

The polymer structure was verified by both ^{1}H NMR and IR spectroscopy. The presence of a peak at 3.67 ppm in the **P1**'s but not in the **P2**'s ^{1}H NMR spectrum indicates OCH_3 protons and the formation of methyl ester groups.[41] From the peak area ratio between the methyl ester protons and the dimethyl group protons of the main chain at around 1 ppm,[41] the percentage of alcoholyzed groups can be estimated to 8% of repeating units. The indices x and y describing the composition of polymer **P1** can be estimated to 30 and 360, respectively (Scheme 1).

dx.doi.org/10.1021/am4015549 | ACS Appl. Mater. Interfaces 2013, 5, 5961–5968

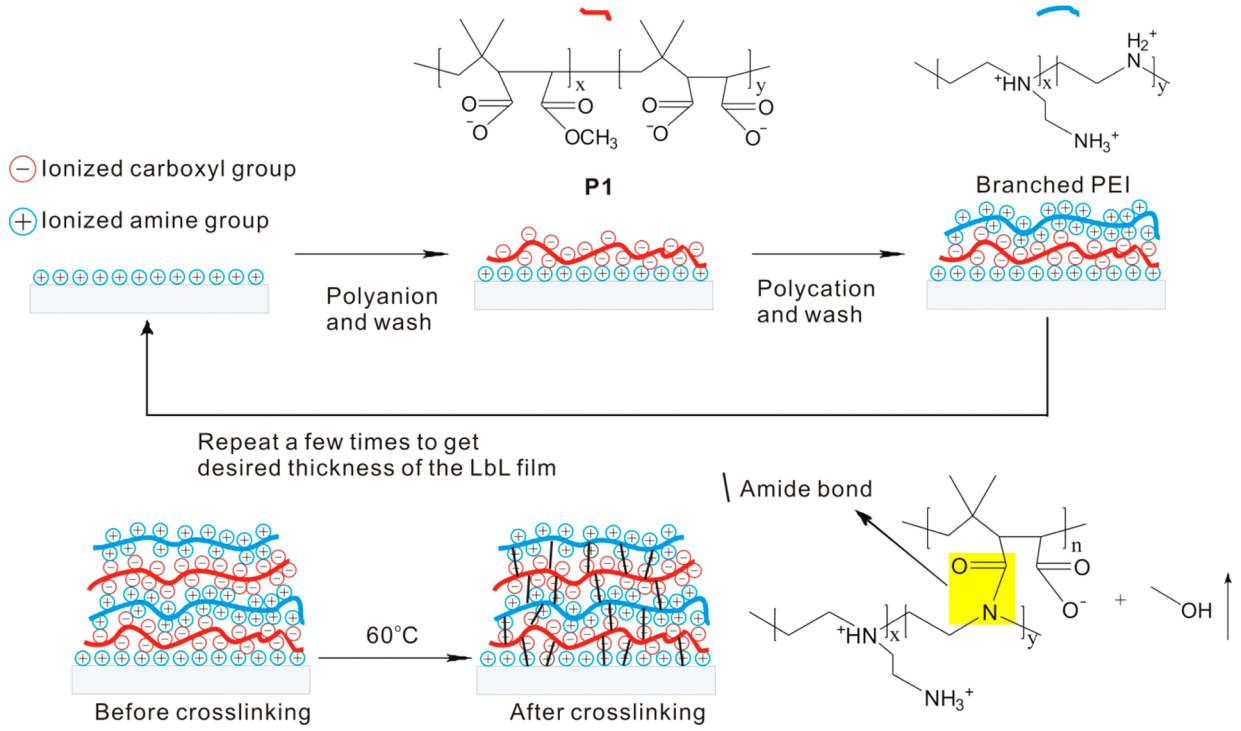

Figure 1. LbL assembly and cross-linking of the deposited polymeric layers.

Additional verification for **P1** and **P2** was provided by FTIR spectra. The double stretching signal $\nu_{C=O}$ (1858 cm^{-1} and 1777 cm^{-1}) belonging to the anhydride is not visible in the FTIR spectrum of **P1** and **P2**, indicating the exhaustive opening of anhydride groups. Ester stretching $\nu_{C=O}$ peak at 1731 cm^{-1} is visible for polymer **P1** indicating the presence of an OCH_3 group. Carboxylic acid stretching peak $\nu_{C=O}$ at around 1580 cm^{-1} is clearly observable for both **P1** and **P2** polymers (see Supporting Information).

3.2. Cross-Linking of the Deposited LbL Assembly. Polyelectrolytes were deposited on pretreated silicon surface from diluted solutions to achieve LbL structure. The assembly of LbL films is mainly driven by a combination of electrostatic interactions and entropy gained from the release of counterions in the solution.[18] The corresponding electrostatic forces are however considered not sufficient to provide high film stability in a harsh environment. As seawater is corrosive, materials used for biofouling prevention require lasting performance, in weeks rather than hours. Hence, a suitable solution for improvement of LbL stability may lie in covalent cross-linking of oppositely charged polymeric layers.

The reported cross-linking methods for LbL assemblies usually need additional chemical treatment,[5] high energy irradiation,[15] or elevated temperature (>100 °C).[27,42] In the proposed LbL system, cross-linking was achieved through a simple aminolysis reaction, which formed an amide covalent bond between polymers **P1** and PEI as shown in Figure 1. Cross-linking is carried out by exposing of the film to temperature of 60 °C and applying vacuum. Under these conditions nucleophilic substitution of methyl ester by amine groups of PEI takes place, and methanol is released in form of vapor, thereby shifting the reaction equilibrium to a higher yield. The aminolysis reaction, among the polyelectrolyte multilayers, was verified by FTIR and XPS spectroscopy of the LbL film before and after treatment. Ester stretching signal $\nu_{C=O}$ at 1727 cm^{-1} (Figure 2a)[41] upon annealing disappears, and a new peak $\nu_{C=O}$ at 1692 cm^{-1} belonging to the amide bond stretching frequency shows up, indicating reaction progress.

The XPS spectra of the LbL films were acquired before and after annealing to verify the cross-linking reaction. In the amidation reaction, the binding energy of C, O, and N atoms would change. The change of XPS spectra of N atom before and after cross-linking was clearly visible due to the high electrowithdrawing effect of carbonyl groups shifting the XPS

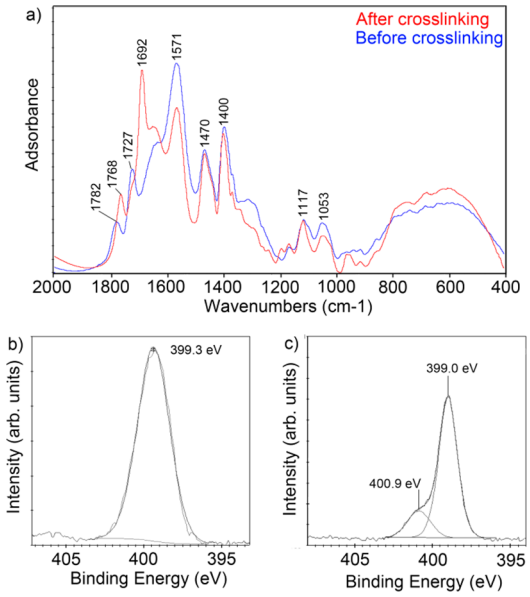

Figure 2. FTIR spectra of the LbL assembly (a) and XPS spectra of the N atom (1 s) of the LbL assembly before (b) and after (c) cross-linking.

dx.doi.org/10.1021/am4015549 | ACS Appl. Mater. Interfaces 2013, 5, 5961−5968

signal to higher energies, as shown in Figure 2b and 2c. Before annealing only 1 peak shows up at 399.3 eV indicating the existence of amine groups connected to the carbon chain. After annealing, in addition to the peak at around 399 eV, a new peak appears at 400.87 eV belonging to the N atom of amide group.[43]

The absence of ester $\nu_{C=O}$ signal from FTIR of cross-linked film and the fact that there is a large excess of amine groups from PEI compared to **P1** ester groups at the polymer interphase within the LbL structure, suggest that the amidation reaction yield is close to quantitative.

3.3. Thickness and Morphology of the Deposited LbL Films. The high control over the thickness of films, constructed with LbL technique, is a great advantage for many applications. It is particularly important when surface chemistry modification is combined with other antifouling strategies, such as surface topological patterning,[9,44] where thickness control is essential to prevent overcoating of patterned features.

In this study, thickness of the built up LbL films was measured by AFM after scratching the surface, as shown in the Supporting Information (Figure S3). The step AFM measurement is a direct and accurate method to detect the multilayer thickness because of direct AFM tip contact with the bare substrate surface and the surface coated with the multilayer.[35] The polyelectrolyte multilayer build up (thickness vs layer number) usually becomes linear after the first few layers.[45] Typically, the thickness of LbL film is controllable only after the initial built up of the adjacent zone to the substrate.[17] The thickness of the polyelectrolyte multilayers in this study was found to grow linearly after the formation of the first five bilayers (Figure 3a).

To evaluate the influence of the cross-linking process on the film morphology, cross-linked and noncross-linked samples were compared. Upon cross-linking the film thickness measured by AFM remained practically unaffected, and only a slight thickness increase was observed (see Figure 4). The surface roughness of the LbL films slightly decreased with the number of bilayers deposited and did not change substantially after deposition of the sixth bilayer. It appears that the deposition of polyelectrolytes may have resulted in a smoother substrate surface given that the initial roughness was not very high. Similar phenomena were reported previoulsy.[46,47] The roughness of the LbL assemblies was also slightly decreased by the cross-linking procedure.

The micelle sizes of the polyelectrolytes in water solution were measured with DLS (Figure 3c), using the same concentrations as for the film deposition. The observable mean diameter of micelles for the PEI solution was much smaller (30 nm) than for the **P1** solution (216 nm). This size variation was also reflected in the bilayer structure, the single layer built up by PEI was thinner than **P1**, as shown in Figure 3b.

The thickness of the LbL films could be controlled by adjusting the number of layers deposited. As mentioned, the deposition of the polyelectrolyte multilayers resulted in a slightly smoother substrate surface (see also roughness data in Figure 4.). This is desirable since a smoother surface can reduce the adhesion of microorganisms such as bacteria in the first stage of biofouling.[11] The mild cross-linking conditions and moderate cross-linking density did not affect the film thickness and film morphology and the resulting layers exhibited smooth and continuous structures.

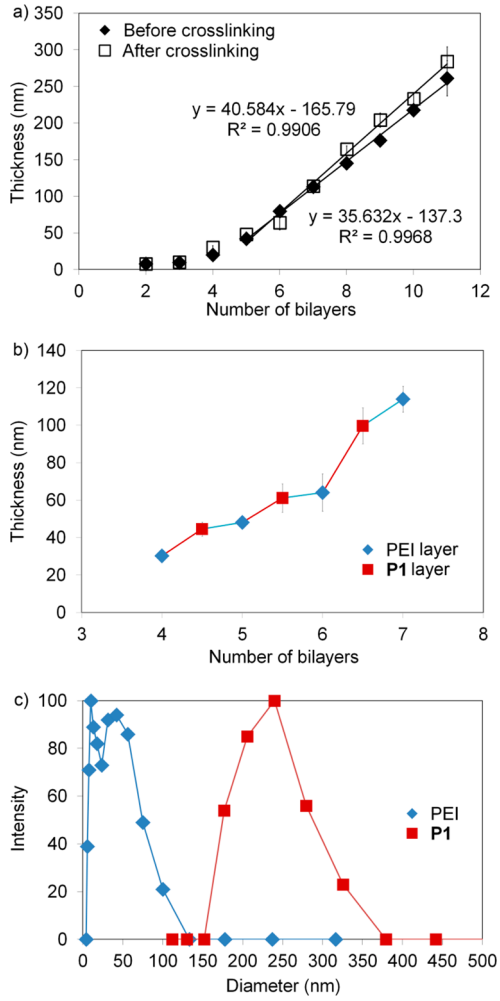

Figure 3. Multilayer thickness measured by AFM. (a) Comparison of thickens evolution with, and without cross-linking of the layers. (b) Thickness increase for positive as well as for negative layer deposited. (c) Distribution of hydrodynamic diameter of polymer aggregates for PEI and **P1** in solution.

3.4. Stability of the LbL Deposited Films. The stability of the noncross-linked LbL electrostatic assembly can be heavily affected by the environmental conditions such as ionic strength, solvent, pH value, etc.[17] In this study, strong covalent bonds were formed among the polyelectrolyte multilayers after cross-linking. The stability of the cross-linked LbL film was evaluated by immersion of substrates in artificial seawater, natural seawater and DMSO.

As shown in Figures 5 and 6, there is a large difference in the properties and behavior between cross-linked and non-cross-linked films of similar chemistry. The non-cross-linked LbL film gradually swelled to about 30% after seven days exposure in artificial seawater (Figure 5a). However, the thickness of the cross-linked LbL film remained unchanged over the same time period. Molecular level swelling was also clearly visible by AFM in the liquid environment (Figure 6).

The roughness value of the LbL film with cross-linking was close to that without cross-linking in dry condition. After exposure to ASW the films swell and their roughness value increases.[48,49] The swelling behavior and observed roughness changes were different in cross-linked and noncross-linked film. As shown in Figure 6, after five days of immersion in ASW, the LbL film without cross-linking achieved roughness values of R_q

dx.doi.org/10.1021/am4015549 | ACS Appl. Mater. Interfaces 2013, 5, 5961−5968

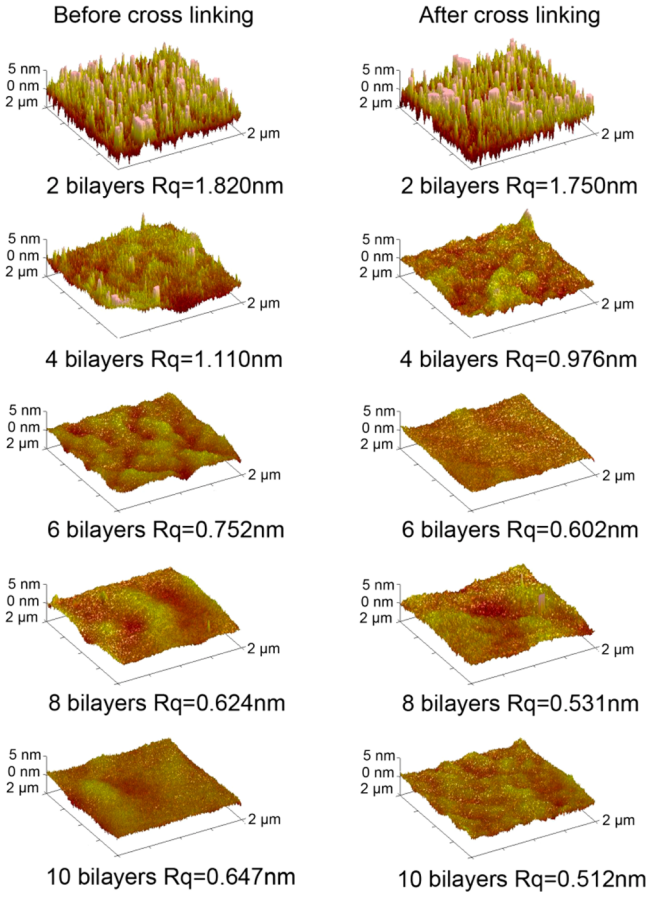

Figure 4. AFM images of the LbL films before (a) and after (b) cross-linking. Rq represents the quadratic mean value of roughness. The scan size was 2 × 2 μm.

= 13.04 nm compare to R_q = 6.58 nm of cross-linked polymer. Since certain amount of salt could penetrate into the LbL film, one may assume that some of the internal ionic bonds could open up, causing the LbL film to swell.[49] After swelling, the LbL films became rougher, weaker and prone to erosion by corrosive chemicals or microorganisms in the marine environment. This was confirmed in experiments conducted in the sea (raft test, Figure 5b). The thickness of the LbL film without cross-linking increased in the first three days, just as had occurred in ASW, but then a quick erosion occurred on the already swollen film over the next few days. On the other hand, the cross-linked film showed much better stability and exhibited only slight change in thickness during the same time period. An interesting phenomenon was observed with the film behavior in a polar organic solvent (DMSO). The thickness of the LbL film without cross-linking dropped to almost 60% after 3 days of immersion in DMSO (Figure 5c). In contrast, no obvious change of the cross-linked LbL film thickness was observed during the 7 d DMSO immersion test. This behavior may be attributed to expelling water from the polar polymeric structure. Upon removal of water and related supporting hydrogen bonds, the polymeric network structure collapsed.

In short, the covalently cross-linked LbL film exhibited enhanced stability in artificial seawater, under field conditions in natural seawater, and in DMSO.

3.5. Antifouling Properties of the LbL films. In the *Amphora* adhesion test (as shown in Figure 7a), more cells were found attached onto the control sample (bare silicon

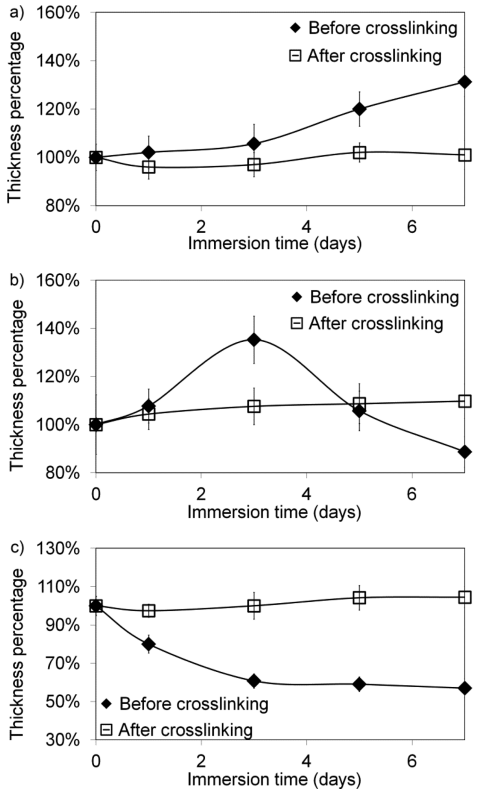

Figure 5. Thickness changes of the LbL films (six bilayers) in (a) artificial seawater, (b) natural seawater, and (c) DMSO immersion tests (measured by AFM in a liquid cell). The solid lines are spline fits to guide the eye. Absolute values of thickness are reported in the Supporting Information.

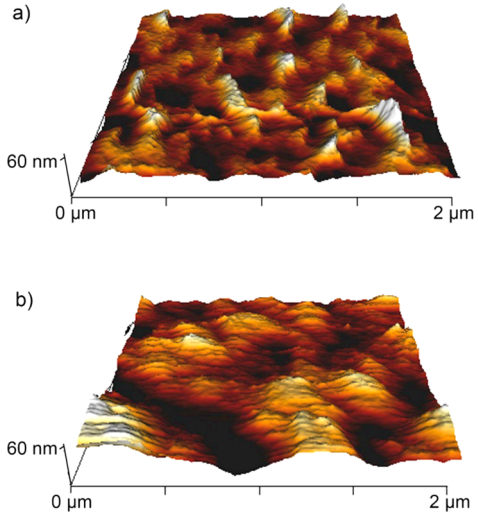

Figure 6. AFM images of the LbL film (six bilayers) without (a, R_q = 13.04 nm) and with (b, R_q = 6.58 nm) cross-linking in artificial seawater after five days immersion (measured by AFM in a liquid cell).

wafer) compared to the substrates with LbL films. The surfaces with the LbL films appear to have slightly better resistance to *Amphora* adhesion than bare silicon. In addition, the attached cell density difference between the cross-linked and noncross-linked films was not significant. In other words, the cross-linking process enhanced the stability of the LbL film without compromising the antiadhesion properties.

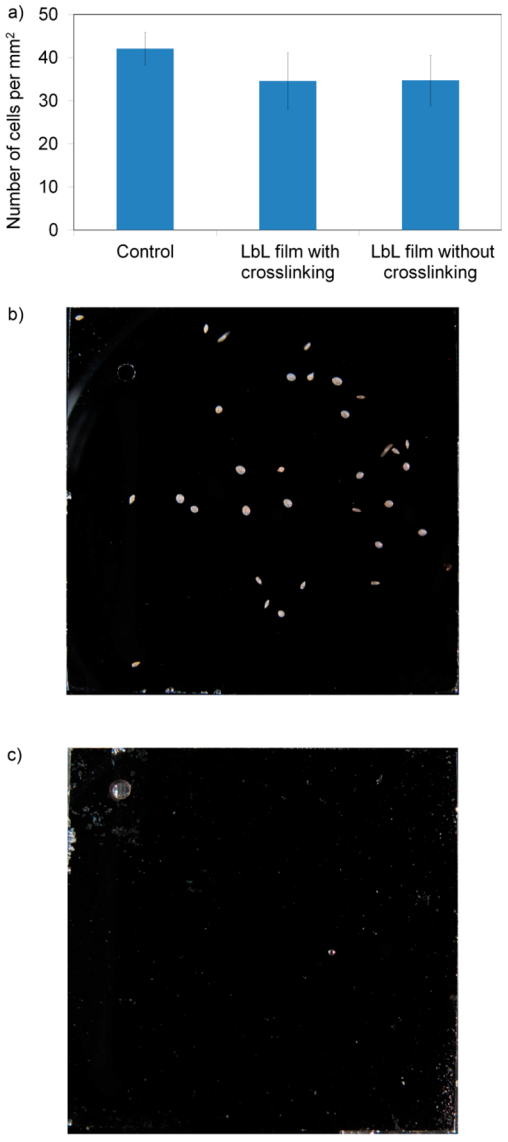

Figure 7. *Amphora* adhesion assays results, error bars given refer to the standard deviation (a); Images of silicon surfaces without (b) and with (c) the LbL film after barnacle cyprid incubation (Size of the coupon is 20 by 20 mm).

Since the LbL films with and without cross-linking provided similar antifouling performance with algae, only the cross-linked LbL film was tested against barnacle cyprids. A total of 119 cyprids were found attached onto the control silicon wafers. However, in sharp contrast, only 17 cyprids were found attached on the 8 replicate silicon wafer surfaces with cross-linked LbL film. Images of the surfaces without and with the LbL film after cyprids incubation were also shown in Figure 7b and 7c.

An antiadhesion effect of the LBL films was observed during settlement of barnacle cyprids. It has been reported that cyprids do not prefer to settle on positively charged surfaces.[50] The built up polyelectrolyte multilayers contain neutral or equally mixed charged bulk layers and a positively charged top layer. This may be one of the reasons why the prepared LbL film with positively charged top layer may have deterred the attachment of cyprids. Finally we note, that positively charged surfaces have also been reported to reduce bacteria attachment and biofilm formation.[14,23]

4. CONCLUSIONS

In this study, we present a novel, robust method for cross-linking of LbL electrostatic assemblies using easily accessible synthetic method to improve stability of the film in harsh marine environments. The presence of amide covalent bonds that serve as cross-linking junctions between polyanion **P1** and PEI was confirmed by FTIR and XPS spectroscopy. In addition, thickness and morphology of the deposited LbL films before and after cross-linking were also studied with AFM. The cross-linking process under mild conditions did not affect the thickness and topography of the deposited LbL films, but dramatically enhanced the stability of them in seawater and in a polar organic solvent (DMSO). In static laboratory tests, the LbL films showed reduced settlement of Amphora and barnacle cyprids adhesion. The proposed method may serve as an efficient approach to cross-link LbL structures containing primary or secondary amines, and would enable the construction of diverse polymeric systems composed of mixed polyelectrolytes for various applications.

■ ASSOCIATED CONTENT

Supporting Information

Additional experimental details and spectra, including FTIR and NMR spectra of the polymers, a figure indicating thickness changes (absolute values) of the LbL films (six bilayers) in artificial seawater, natural seawater and DMSO immersion tests, a figure indicating thickness measurement of LbL film through AFM method, and a table showing the thickness data of LbL films with different bilayers. This material is available free of charge via the Internet at http://pubs.acs.org.

■ AUTHOR INFORMATION

Corresponding Author

*Tel: +65 6874 5443 (D.J.); +31 53 489 2974 (G.J.V.). Fax: +65 6872 0785 (D.J.); +31 53 4893823 (G.J.V.). E-mail: janczewskid@imre.a-star.edu.sg (D.J.); g.j.vancso@utwente.nl (G.J.V.).

Notes

The authors declare no competing financial interest.

■ ACKNOWLEDGMENTS

The authors are grateful to the Agency for Science, Technology and Research (A*STAR) for providing financial support under the Innovative Marine Antifouling Solutions (IMAS) program.

■ REFERENCES

(1) Callow, J. A.; Callow, M. E. *Nat. Commun.* **2011**, *2*, 244.
(2) Lejars, M.; Margaillan, A.; Bressy, C. *Chem. Rev.* **2012**, *112*, 4347−4390.
(3) Abarzua, S.; Jakubowski, S. *Mar. Ecol.: Prog. Ser.* **1995**, *123*, 301−312.
(4) Schultz, M. P.; Bendick, J. A.; Holm, E. R.; Hertel, W. M. *Biofouling* **2011**, *27*, 87−98.
(5) Cao, S.; Wang, J. D.; Chen, H. S.; Chen, D. R. *Chin. Sci. Bull.* **2011**, *56*, 598−612.
(6) Callow, M. E.; Callow, J. A. *Biologist* **2002**, *49*, 10−14.
(7) Banerjee, I.; Pangule, R. C.; Kane, R. S. *Adv. Mater.* **2011**, *23*, 690−718.
(8) Krishnan, S.; Weinman, C. J.; Ober, C. K. *J. Mater. Chem.* **2008**, *18*, 3405−3413.
(9) Schumacher, J. F.; Long, C. J.; Callow, M. E.; Finlay, J. A.; Callow, J. A.; Brennan, A. B. *Langmuir* **2008**, *24*, 4931−4937.
(10) Scardino, A. J.; de Nys, R. *Biofouling* **2011**, *27*, 73−86.

(11) Verran, J.; Boyd, R. D. *Biofouling* **2001**, *17*, 59−71.
(12) Lindner, E. *Biofouling* **1992**, *6*, 193−205.
(13) Yang, W. J.; Neoh, K. G.; Kang, E. T.; Lee, S. S. C.; Teo, S. L. M.; Rittschof, D. *Biofouling* **2012**, *28*, 895−912.
(14) Zhao, Y. H.; Zhu, X. Y.; Wee, K. H.; Bai, R. *J. Phys. Chem. B* **2010**, *114*, 2422−2429.
(15) Kuo, W. H.; Wang, M. J.; Chien, H. W.; Wei, T. C.; Lee, C.; Tsai, W. B. *Biomacromolecules* **2011**, *12*, 4348−4356.
(16) Jiang, S.; Cao, Z. *Adv. Mater.* **2010**, *22*, 920−932.
(17) Decher, G.; Schlenoff, J. B. *Multilayer Thin Films: Sequential Assembly of Nanocomposite Materials*; Wiley-VCH: Weinheim, Germany, 2003; p 524.
(18) von Klitzing, R. *Phys. Chem. Chem. Phys.* **2006**, *8*, 5012−5033.
(19) Izquierdo, A.; Ono, S. S.; Voegel, J. C.; Schaaf, P.; Decher, G. *Langmuir* **2005**, *21*, 7558−7567.
(20) Ma, Y.; Dong, W. F.; Hempenius, M. A.; Mohwald, H.; Vancso, G. J. *Nat. Mater.* **2006**, *5*, 724−729.
(21) Song, J.; Janczewski, D.; Ma, Y.; Hempenius, M.; Xu, J.; Vancso, G. J. *J. Mater. Chem. B* **2013**, *1*, 828−834.
(22) Antipina, M. N.; Sukhorukov, G. B. *Adv. Drug Delivery Rev.* **2011**, *63*, 716−29.
(23) Lichter, J. A.; Rubner, M. F. *Langmuir* **2009**, *25*, 7686−7694.
(24) Lichter, J. A.; Van Vliet, K. J.; Rubner, M. F. *Macromolecules* **2009**, *42*, 8573−8586.
(25) Cortez, C.; Quinn, J. F.; Hao, X.; Gudipati, C. S.; Stenzel, M. H.; Davis, T. P.; Caruso, F. *Langmuir* **2010**, *26*, 9720−9727.
(26) Yang, W. J.; Pranantyo, D.; Neoh, K. G.; Kang, E. T.; Teo, S. L. M.; Rittschof, D. *Biomacromolecules* **2012**, *13*, 2769−80.
(27) Cao, X.; Pettitt, M. E.; Wode, F.; rpa Sancet, M. P.; Fu, J.; Ji, J.; Callow, M. E.; Callow, J. A.; Rosenhahn, A.; Grunze, M. *Adv. Funct. Mater.* **2010**, *20*, 1984−1993.
(28) Liu, T.; Yin, B.; He, T.; Guo, N.; Dong, L.; Yin, Y. *ACS Appl. Mater. Interfaces* **2012**, *4*, 4683−4690.
(29) Wang, F.; Feng, J.; Gao, C. *Colloid Polym. Sci.* **2008**, *286*, 951−957.
(30) Olivier, F.; Tremblay, R.; Bourget, E.; Rittschof, D. *Mar. Ecol.: Prog. Ser.* **2000**, *199*, 185−204.
(31) Rasmussen, K.; Østgaard, K. *Biofouling* **2001**, *17*, 103−115.
(32) Phang, I. Y.; Aldred, N.; Ling, X. Y.; Huskens, J.; Clare, A. S.; Vancso, G. J. *J. R. Soc. Interface* **2010**, *7*, 285−296.
(33) Phang, I. Y.; Chaw, K. C.; Choo, S. S. H.; Kang, R. K. C.; Lee, S. S. C.; Birch, W. R.; Teo, S. L. M.; Vancso, G. J. *Biofouling* **2009**, *25*, 139−147.
(34) Phang, I. Y.; Aldred, N.; Clare, A. S.; Callow, J. A.; Vancso, G. J. *Biofouling* **2006**, *22*, 245−250.
(35) Lefaux, C. J.; Zimberlin, J. A.; Dobrynin, A. V.; Mather, P. T. *J. Polym. Sci., Part B: Polym. Phys.* **2004**, *42*, 3654−3666.
(36) Holland, R.; Dugdale, T. M.; Wetherbee, R.; Brennan, A. B.; Finlay, J. A.; Callow, J. A.; Callow, M. E. *Biofouling* **2004**, *20*, 323−329.
(37) Guillard, R. R.; Ryther, J. H. *Can. J. Microbiol.* **1962**, *8*, 229−239.
(38) Willemsen, P. R.; Overbeke, K.; Suurmond, A. *Biofouling* **1998**, *12*, 133−147.
(39) Marechal, J. P.; Hellio, C. *Int. Biodeterior. Biodegrad.* **2011**, *65*, 92−101.
(40) Janczewski, D.; Tomczak, N.; Han, M. Y.; Vancso, G. J. *Nat. Protoc.* **2011**, *6*, 1546−1553.
(41) Pretsch, E.; Bnhlmann, P.; Affolter, C. *Structure Determination of Organic Compounds*; Springer: Berlin, 2009.
(42) Jang, W. S.; Jensen, A. T.; Lutkenhaus, J. L. *Macromolecules* **2010**, *43*, 9473−9479.
(43) Moulder, J. F.; Chastain, J. *Handbook of X-ray Photoelectron Spectroscopy: A Reference Book of Standard Spectra for Identification and Interpretation of XPS Data*; Perkin-Elmer Corporation: Eden Prairie, MN, 1992; p 259.
(44) Schumacher, J. F.; Carman, M. L.; Estes, T. G.; Feinberg, A. W.; Wilson, L. H.; Callow, M. E.; Callow, J. A.; Finlay, J. A.; Brennan, A. B. *Biofouling* **2007**, *23*, 55−62.
(45) Schlenoff, J. B.; Dubas, S. T. *Macromolecules* **2001**, *34*, 592−598.
(46) Zhang, L.; Vidu, R.; Waring, A. J.; Lehrer, R. I.; Longo, M. L.; Stroeve, P. *Langmuir* **2002**, *18*, 1318−1331.
(47) Kim, Y. H.; Lee, Y. M.; Park, J.; Ko, M. J.; Park, J. H.; Jung, W.; Yoo, P. J. *Langmuir* **2010**, *26*, 17756−17763.
(48) Vogt, B. D.; Lin, E. K.; Wu, W. L.; White, C. C. *J. Phys. Chem. B* **2004**, *108*, 12685−12690.
(49) Sukhorukov, G. B.; Schmitt, J.; Decher, G. *Phys. Chem. Chem. Phys.* **1996**, *100*, 948−953.
(50) Petrone, L.; Di Fino, A.; Aldred, N.; Sukkaew, P.; Ederth, T.; Clare, A. S.; Liedberg, B. *Biofouling* **2011**, *27*, 1043−1055.